Effect of SiC Content on the Microstructure and Properties of $Zr_2Al_4C_5$/SiC Composites in situ Fabricated by Spark Plasma Sintering

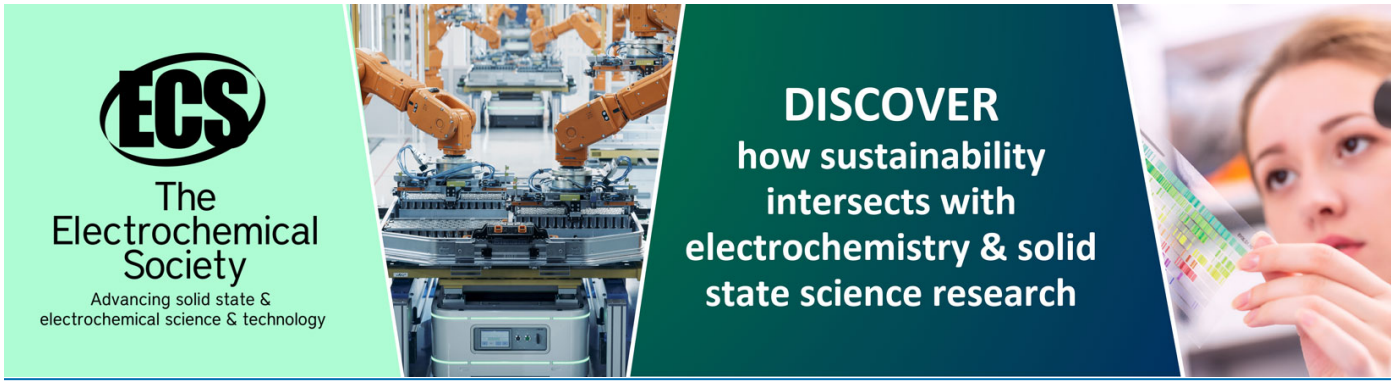

IOP Conf. Series: Materials Science and Engineering **678** (2019) 012073 doi:10.1088/1757-899X/678/1/012073

Effect of SiC Content on the Microstructure and Properties of $Zr_2Al_4C_5$/SiC Composites in situ Fabricated by Spark Plasma Sintering

Qilong Guo[1, 2,*], Jing Wang [1], Junjun Pei [1], Junguo Li [2], and Lianmeng Zhang [2]

[1]Key Laboratory of New Building Materials and Building Energy Efficiency of Gansu Province, School of Civil Engineering, Northwest Minzu University, Lanzhou 730124, P. R. China

[2]State Key Lab of Advanced Technology for Materials Synthesis and Processing, Wuhan University of Technology, Wuhan 430070, P. R. China

Corresponding author:guoqilong8@126.com.

Abstract. $Zr_2Al_4C_5$/SiC composite ceramics were successfully fabricated from the powder mixture of Zr, Al, C and SiC by spark plasma sintering method. The composition-dependent densification, phase evolution, microstructure and mechanical properties of the composite ceramics were studied. With increasing the SiC content in the starting powder mixture, the densification behavior of sintered samples was promoted. It is found that the as-sintered products are mainly composed of $Zr_2Al_4C_5$ matrix and SiC reinforcement, and the fine SiC particles tend to disperse on the matrix grain boundaries. Besides, the addition of SiC particles can evidently hinder the coarsening of $Zr_2Al_4C_5$ grains. Both the Vickers hardness and Young's modulus of composites ceramics gradually increase as increasing the SiC content. The fracture toughness of the composites decreases first then increases with the increase in the SiC and the $Zr_2Al_4C_5$/30vol%SiC sample possesses the maximum value of 4.4MPa·$m^{1/2}$.

1. Introduction

Compared with the corresponding binary carbide ZrC, the Zr-Al-C compounds (including $Zr_2Al_4C_5$, $Zr_3Al_4C_6$ and $Zr_2Al_3C_5$)show superior oxidation resistance, high fracture toughness, and excellent room and high-temperature stiffness, being promising high-temperature structure ceramics[1-4]. The Zr-Al-C compounds also exhibit comparable high-temperature mechanical properties, the Young's modulus decreased slowly with increasing temperature and the Young's modulus was 293 GPa at 1580 °C, which is about 81% of that at room temperature. At the same time, the strength at 1400 °C was 371 MPa, which is about 10% higher than that at room temperature. These properties make it attractive candidate for high-temperature structural applications in aerospace.

However, as a high-temperature structural material, the fracture toughness, hardness and oxidation resistance of $Zr_2Al_4C_5$ ceramics at high temperature is still unsatisfactory, which restrict its wider application. Recently, a number of works have been published on improving the mechanical properties of $Zr_2Al_4C_5$. Owing to the light weight, high hardness and strength, superior high temperature oxidation resistance[5-6], the incorporation of second phase SiC particles into $Zr_2Al_4C_5$ significantly improve the hardness, fracture toughness, and oxidation resistance[7-8]. However, to the best of the

authors' knowledge, few studies have been carried out on the composition (SiC volume contents)-dependent mechanical properties of $Zr_2Al_4C_5$/SiC composite ceramics in the open literature.

In the present work, therefore, the $Zr_2Al_4C_5$/SiC composites were prepared using Zr, Al, graphite, and SiC powders as initial materials by spark plasma sintering process. The effect of SiC content on the densification, phase evolution, microstructure and mechanical properties of the composites were investigated in detail. The related mechanism was also discussed.

2. Experimental procedures

Commercially available powders of Zr (99.9%, 10 μm, Beijing mountain technical development center for non-ferrous metals, China), Al (99.99%, 8 μm, Shanghai chemical reagents of Chinese medicine group, China), graphite (99.9%, 1 μm, Shanghai capable graphite Co. Ltd., China), and SiC (99.5%, 5μm, Weifang Kaihua Micro-powder Co. Ltd., China) were selected as raw materials for the synthesis of $Zr_2Al_4C_5$/SiC composites.

The molar ratios of starting powders were selected to 2Zr/6.2Al/4.8C, in order to compensate the loss of Al at higher temperatures, off-stoichiometry molar content of Al were used. Finally, the $Zr_2Al_4C_5$/SiC composites with 0 vol%, 10 vol%, 20 vol% and 30 vol% SiC were obtained and designated as ZS0~ZS3, respectively.

The mixture of initial powders with the designed composition was mixed in an agate mortar, and put into graphite crucibles of 15 mm in diameter and finally spark plasma sintered in vacuum (model-1050, Sumitomo Coal Mining Co. Ltd., Tokyo), under a temperature of 1800 ◦C for 3 min with a uniaxial pressure of 20 MPa. The temperature was measured by means of an optical pyrometer focused on to the sintered sample through a small hole in the die. The detailed operation and sintering process of spark plasma sintering (SPS) was reported in the previous papers[9-10].

The open porosity of the sintered products was determined by Archimedes' immersion method with water as the immersing medium. The microstructure of ceramic samples was studied by using X-ray diffraction (XRD, X'Pert PRO-PANalytical) with Cu Kα radiation. The polished surface and fracture morphologies of sintered ceramic samples and the surface and cross-sectional morphologies of the samples after high-temperature oxidation were observed by using scanning electron microscope (SEM). The grain sizes of samples were determined from SEM images using the average of length and width from 50 randomly selected grains. The testing details of the Young's modulus (E), the Vickers hardness and fracture toughness of the ceramic samples were reported in the previous papers[9-10].

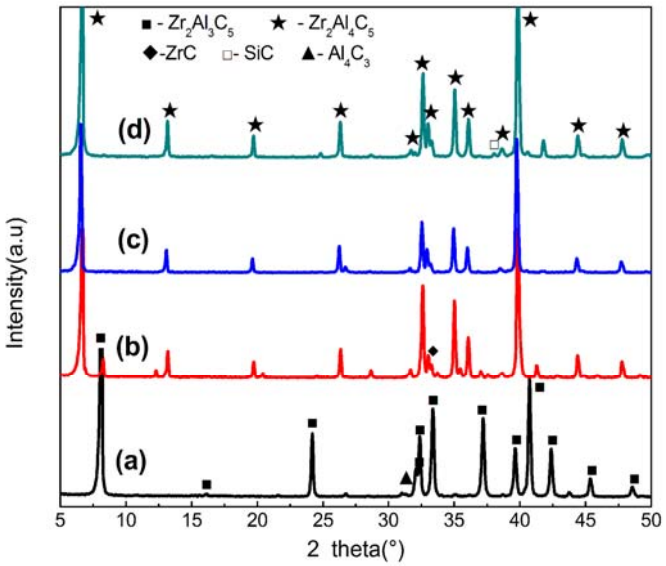

Figure 1. the XRD patterns of the composites: (a) ZS0, (b) ZS1, (c) ZS2, (d) ZS3.

3. Results and discussion

Figure 1 shows the XRD patterns of the composites. As shown in Figure 1(a), the peaks of $Zr_2Al_4C_5$ was not detected in the SPS sintered sample, and the main peaks were related to the $Zr_2Al_3C_5$ phase. However, with the increase of the content of SiC, only a traces amount of $Zr_2Al_3C_5$ was detected, besides the main phase of $Zr_2Al_4C_5$, which indicates SiC played a key role on the synthesis of $Zr_2Al_4C_5$[11].

The density and open porosity of samples sintered at 1800 ^oC for 3 min as a function of SiC content is shown in table 1. The density of $Zr_2Al_4C_5$/SiC composite gradually decreases with the content of SiC increasing. The density increases due to a smaller density of 4.5 g/cm^3 for $Zr_2Al_4C_5$ than that of 3.22 g/cm^3 for SiC[2, 6]. It can be seen that the open porosity decreased with the increase of SiC volume content and all the composite ceramics have much lower open porosities only around 0.06-0.21%, indicating that the desification of the composite ceramics are easier to achieve due to the existence of SiC which is densified.

Table 1. Open porosity, aspect ratio of $Zr_2Al_4C_5$ grains, Vickers hardness and Young's modulus of samples with different SiC volume contents

Samples	Density (g/cm^3)	Open porosity (%)	Diameter of elongated grains (μm)	Aspect ratio of $Zr_2Al_4C_5$ grains	Vickers' hardness (GPa)	Young's modulus (GPa)
0vol%	4.3121	0.21	2.85±0.25	4.10±0.94	10.6±0.3	320±20
10vol%	4.2076	0.17	3.68±0.45	3.15±0.85	11.0±0.3	340±30
20vol%	4.0392	0.11	3.28±0.35	4.05±1.05	12.7±0.4	355±25
30vol%	4.0108	0.06	2.35±0.45	4.35±1.15	15.0±0.4	365±25

Table 1 compares the diameter and aspect ratio of elongated $Zr_2Al_4C_5$ grains for $Zr_2Al_4C_5$/SiC samples. The aspect ratio of Zr-Al-C grains of pure Zr-Al-C ceramic is 4.10 ± 0.94. As the volume content of Zr-Al-C decreases from 90 vol.% to 70 vol.%, the aspect ratio of Zr-Al-C first decreases from 3.15 ± 0.85 for ZS1 and then apparently increases to 4.35±1.15 for ZS3. With the increase of SiC content, the diameter of elongated $Zr_2Al_4C_5$ grains decreased as a consequence of the pinning effect of SiC on the grain-boundary. As discussed above, the grain size of $Zr_2Al_4C_5$ matrix decreases with the increase in the SiC content, which suggests that the addition of SiC particles can evidently hinder the coarsening of Zr-Al-C grains, and the restriction in grain growth could further improve the densification and the material's stability at elevated temperature during sintering [12].

Vickers hardness and Young's modulus of Zr-Al-C-based composite as function of SiC content are listed in Table 1. It can be seen that the Vickers hardness and Young's modulus increase gradually with the increase of SiC volume content. Compared to ZrB_2 and SiC, $Zr_2Al_4C_5$ has a low hardness of about 11 GPa [3], the incorporation of SiC could effectively improve the Vickers hardness of the composites. The intrinsic Young's modulus of SiC was higher than Zr-Al-C. In addition, the ceramics with the lowest porosity and lower grain size of the matrix. The ZS3 sample exhibits relatively higher values of Vickers' hardness and Young's modulus.

Figure 2 shows the polished surface morphologies from SEM backscattered electron images of samples with different compositions of Zr-Al-C and SiC volume contents. It is clearly observed that there are two distinct phases which have different grain shape and sizes. Combining with the analysis of XRD and EDS (not shown), the columnar or plate-like gray grains are identified as Zr-Al-C grains and the dark particles are SiC grains. As shown in the figures, the SiC particles disperse homogenously among the Zr-Al-C grains, which was helpful to reinforce the mechanical properties. The matrix grain size of the products decreases significantly as the SiC content increase, and no any pore could be observed in the SiC containing composites.

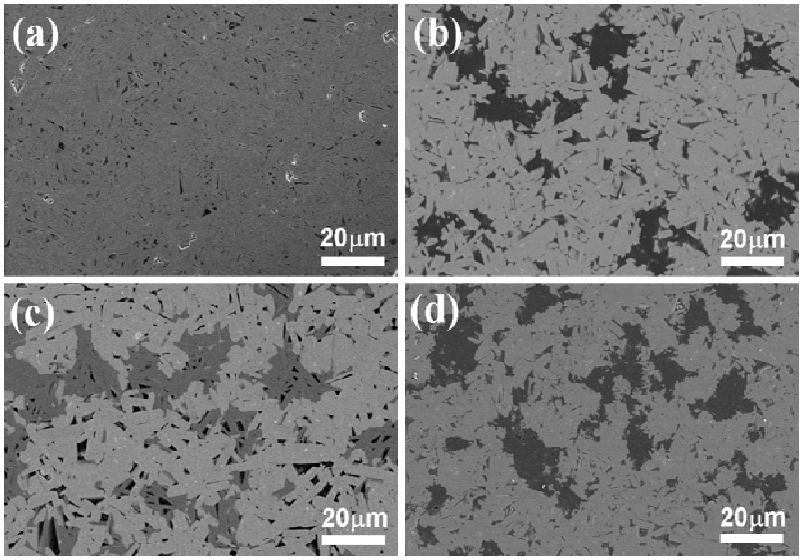

Figure 2. BESEM images of the polished surfaces of composite ceramics: (a) ZS0, (b) ZS1, (c) ZS2, (d) ZS3.

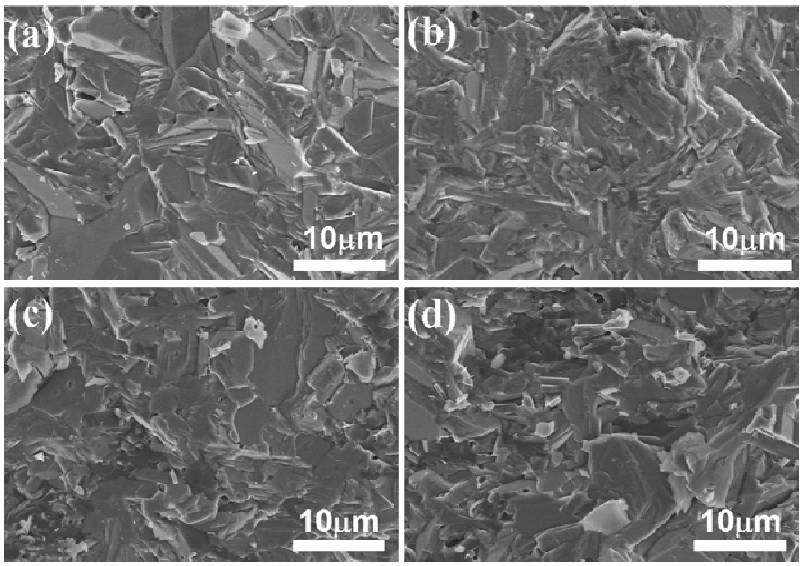

Figure 3. the features of fractured surfaces of the composites with different SiC content: (a) ZS0, (b) ZS1, (c) ZS2, (d) ZS3.

Figure 3 shows the SEM fractured surfaces of samples with different compositions of Zr-Al-C and SiC volume contents. As shown in the figures, the pure Zr-Al-C ceramic and all the $Zr_2Al_4C_5$/SiC composite ceramics are almost densified and pores are hardly observed. It can be seen that the mode of fracture of monolithic Zr-Al-C is transgranular, wherever the grain size is large, and therefore the fracture surface is flat, as shown in Figure 3(a). The fracture surfaces of $Zr_2Al_4C_5$/SiC composite ceramic samples are relatively rough and exhibit an evident combination fraction mode of inter-granular and trans-granular fracture as shown in Figure 3(b)-3(d).

The fracture toughness values of the compositions are depicted in Figure4. The fracture toughness of $Zr_2Al_4C_5$/SiC composite ceramics firstly decreases and then increases with increasing the SiC content. Among them, the composites reinforced with 30 vol% SiC exhibited the highest fracture toughness of 4.4 ± 0.18 MPa·$m^{1/2}$. It can be seen from Table 1 that the maximum average aspect ratio of Zr-Al-C grains was estimated to be 4.35±1.15 for ZS3.It is generally believed that elongated grains

with large aspect ratio benefit the fracture toughness of ceramic matrix[10].In addition, the higher fracture toughness of ZS3 is attributed to the relatively finer and homogeneous microstructure, as shown in Figure 3 (d).

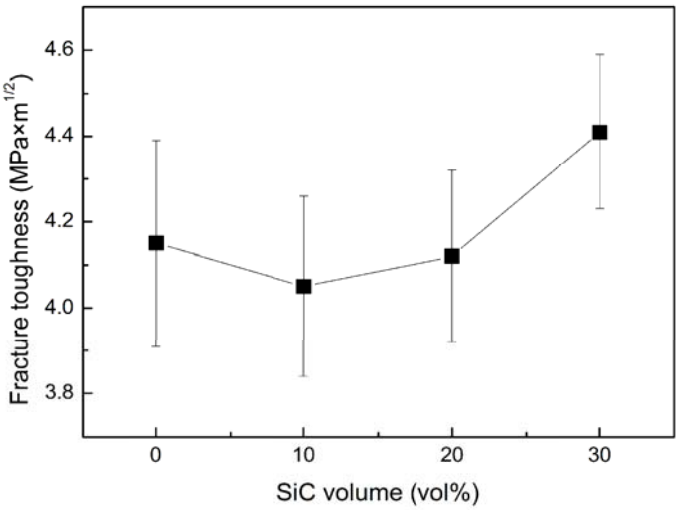

Figure 4. The fracture toughness values of multiphase ceramics with different volume contents of SiC

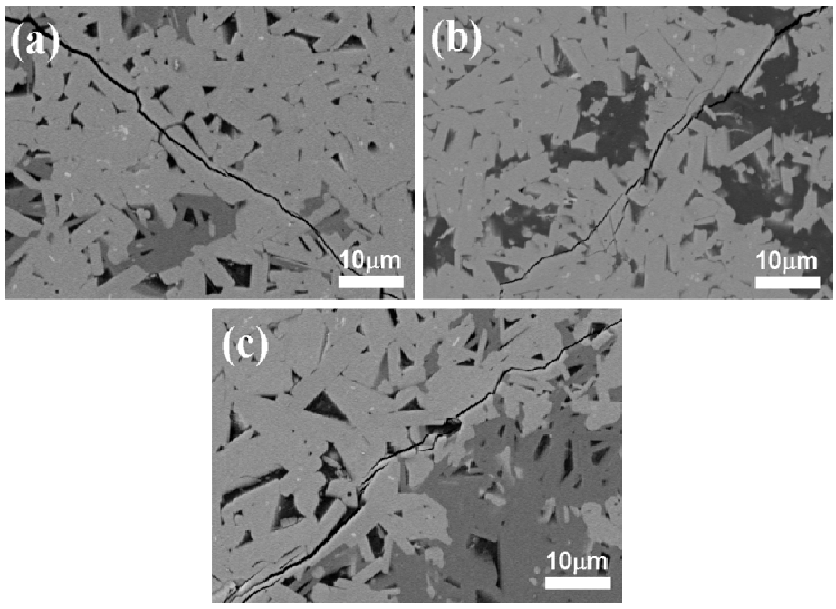

Figure 5. Propagation path of the $Zr_2Al_4C_5$/SiC composite ceramics: (a) ZSO, (b) ZS2 and (c) ZS3.

In order to elucidate the mechanism in composition-dependent fracture toughness of samples with different compositions of Zr-Al-C and SiC volume contents, the crack propagation features of all sintered ceramic samples are observed through SEM surface morphology images shown in Figure5. Compared to ZS0 samples, in the $Zr_2Al_4C_5$/SiC composite ceramic samples the crack path is zigzag and prolonged due to the combination of trans-granular and inter-granular fracture, indicating that these interactions absorb the energy of crack propagation during the fracture process and lead to more shorter crack paths for toughening the composite ceramics[13], which is evident shown in Figure 5(b)-5(c) and agrees well with the results from fracture morphologies shown in Figure 3(d). Furthermore,

inspection of crack propagation reveals that the crack deflection and crack bridging are caused by the layer-structured Zr-Al-C grains.

4. Conclusions

$Zr_2Al_4C_5$/SiC composites were synthesized by the in situ reactive spark plasma sintering at 1800 ◦C for 3 min under 20MPa. The addition of SiC resulted in significant decrease in open porosity of the ceramics. It is found that the as-sintered products are mainly composed of $Zr_2Al_4C_5$ matrix and SiC reinforcement, the SiC particles disperse uniformly throughout of the matrix $Zr_2Al_4C_5$. The addition of SiC particles can evidently hinder the coarsening of $Zr_2Al_4C_5$ grains, and the fracture exhibited a combination mode of intergranular and transgranular propagation. The introduction of SiC increases the Vickers hardness and Young's modulus of $Zr_2Al_4C_5$/SiC composites gradually increase. The fracture toughness of the composites decreases first then increases with the increase in the SiC and the $Zr_2Al_4C_5$/30vol%SiC sample possesses the maximum value of 4.4 MPa·$m^{1/2}$.

Acknowledgement

This work was financially supported by the Fundamental Research Funds for the Central Universities of Northwest Minzu University (31920180019). The project supported by State Key Laboratory of Advanced Technology for Materials Synthesis and Processing (Wuhan University of Technology) (2019-KF-7). And the research work was also supported by the Special Funds for Introducing Talents from Northwest Minzu University (Z14013).

References

[1] Lin Z J, He L F, Wang J Y, Li M S, Bao Y W, and Zhou Y C 2008*Acta Mater*. **56** 2022
[2] He L F, Bao Y W, Wang J Y, Li M S, and Zhou Y C 2009*J. Am. Ceram. Soc.***92** 445
[3] He L F, Lu X P, Bao Y W, Wang J Y, and Zhou Y C 2009*Scr. Mater.***61** 60
[4] Zhou Y C, He L F, Lin Z J, Wang J Y 2013 *J. Eur. Ceram. Soc.***33** 2831
[5] Bhattacharya AK and Petrovic JJ 1991 *J. Am. Ceram. Soc.***90** 2700
[6] Chamberlain AL, FahrenholtzWG and Hilmas GE2004*J. Am. Ceram. Soc.***87**1170
[7] Chen G Q, Zhang R B, Hu P and Han W B 2009*Scr. Mater.***61** 697
[8] He L F, Li F Z, Lu X P, Bao Y W, and Zhou Y C 2010*J. Eur. Ceram. Soc.***30** 2147
[9] Guo Q L, Li J G, Shen Q,and Zhang L M 2012*Mater. Sci. Eng.A.***558** 186
[10] Guo Q L, Luo S J, Gan J Z, Li J G,and Zhang L M 2015 *Mater. Sci. Eng.A.***644**96
[11] He LF, Zhou YC, Bao YW, Lin ZJ, and Wang JY 2007*J. Am. Ceram. Soc.***90**1164
[12] Tadokoro SK and Muccillo ENS2002*J. Eur. Ceram. Soc.***22** 1723
[13] Rodel J 1992*J. Eur. Ceram. Soc.***10** 143